

**Nonadiabatic holonomic quantum computation in decoherence-free subspaces with trapped ions**Zhen-Tao Liang, Yan-Xiong Du, Wei Huang, Zheng-Yuan Xue,<sup>\*</sup> and Hui Yan<sup>†</sup>*Laboratory of Quantum Engineering and Quantum Materials, School of Physics and Telecommunication Engineering, South China Normal University, Guangzhou 510006, China*

(Received 21 January 2014; published 10 June 2014)

Implementing nonadiabatic holonomic quantum computation in decoherence-free subspaces may consolidate the advantages of both strategies and thus leads to suppression of both local and collective noises. In a recent paper, Xu *et al.* [*Phys. Rev. Lett.* **109**, 170501 (2012)] proposed an interesting implementation of such a scheme; however, four-body interaction, which is hard to achieve in a realistic system, is required there. In this paper we propose a simplified scheme to implement such single-qubit and two-qubit logical operations by utilizing only two-body interactions, which is much easier to realize in a trapped ion system.

DOI: [10.1103/PhysRevA.89.062312](https://doi.org/10.1103/PhysRevA.89.062312)

PACS number(s): 03.67.Pp, 03.65.Vf

**I. INTRODUCTION**

The physical implementation of quantum computation presents an unprecedented challenge right now. The main practical difficulties are the decoherence effect caused by the control errors as well as the unwanted couplings with environments. Usually, the sources of decoherence can be divided into local and collective noises. Geometric phases depend only on some global geometric features of the evolution path and are largely insensitive to local noises. Therefore, geometric phases have been used in quantum computation [1–8] as well as other quantum manipulation [9] to robust against local noises and fluctuations. Interestingly, high-fidelity geometric quantum gates (which are realized with pure geometric phases) have been experimentally realized by several groups [10–12]. Quantum computation based on geometric phases is usually classified into two categories [1]. One is geometric quantum computation (GQC) [4–8], where quantum gates are based on Abelian geometric phases. The other one is holonomic quantum computation (HQC) [2,3,13–16], which is based on degenerated non-Abelian holonomy. Both categories of quantum computation have been experimentally realized and provide promising approaches to suppress the local fluctuations.

On the other hand, collective noises may be caused by the interaction between a quantum system and its environment, which possesses some symmetries. To suppress such collective noises, schemes based on the decoherence-free subspaces (DFSs) were proposed [17–19]. In addition, DFSs have been experimentally realized in many physical systems [20–24].

To protect quantum information from both local and collective errors, schemes combining GQC or HQC with DFSs in an adiabatic scenario have been proposed [25,26]. However, the adiabatic condition requires that the gate time must be longer than a characterized time of the qubit system, which is usually comparable with the coherence time [4,5]. In order to avoid the dilemma between long run time and limited coherence time in adiabatic HQC, nonadiabatic holonomic quantum computation (NHQC) protocols have been proposed [27,28]. Robust elementary gate operations have also been

experimentally verified recently [11,12]. Very recently, in order to avoid the long run-time requirement, Xu *et al.* [29] proposed an interesting strategy by combining the NHQC with a three-qubit encoding DFS to realize universal quantum computation. However, the proposal requires four-body interactions to achieve the effective quantum gate, which is very challenging since there is no direct way to implement such interactions in a realistic physical system.

In this paper, we use the trapped-ion system as a detailed example to show that two-body pairwise effective exchange interactions are sufficient to realize universal quantum computation with the combination of NHQC and DFSs. Meanwhile, DFSs have also been tested with the trapped-ion system [30]. Therefore, our scheme provides a simplified implementation of NHQC in DFSs, and in principle can be realized with trapped ions, which is one of the leading candidates for quantum computation [31].

The rest of this paper is arranged as follows. In Sec. II we briefly describe the physical system of ion traps and the effective exchange interactions in ion traps. In Sec. III, we show how the effective exchange interactions can be used to efficiently perform single-logical qubit holonomic gates using a three-qubit encoding into a collective dephasing DFS. In Sec. IV, we show how the effective exchange interactions can be used to efficiently perform two-logical qubit holonomic gates within the chosen DFS. In Sec. V, we present a conclusion of our scheme.

**II. EFFECTIVE INTERACTIONS**

We consider a string of  $N$  two-level ions in a linear trap, which can be individually addressed by bichromatic laser fields. Each logical qubit consists of three ions. As shown in Fig. 1(a), ions 1,2,3 (4,5,6) represent the logical qubit 1 (2). Two groups of lasers are utilized. As shown in Fig. 1(b), the first group consists of two laser fields, with frequencies  $\omega_0 + (\nu + \delta)$  (phase  $\phi_i$ ). Here  $\omega_0$  is the resonant frequency between the two energy states  $|1\rangle$  and  $|0\rangle$  of the ions;  $\nu$  is the frequency of vibrational mode and  $\delta$  is an additional detuning;  $i$  is the subscript labeling the ions.

When two ions, i.e., ions 1 and 2, are interacting with the above laser fields simultaneously, also assuming  $\delta \ll \nu$ , the

<sup>\*</sup>zyxue@scnu.edu.cn<sup>†</sup>yanhui@scnu.edu.cn

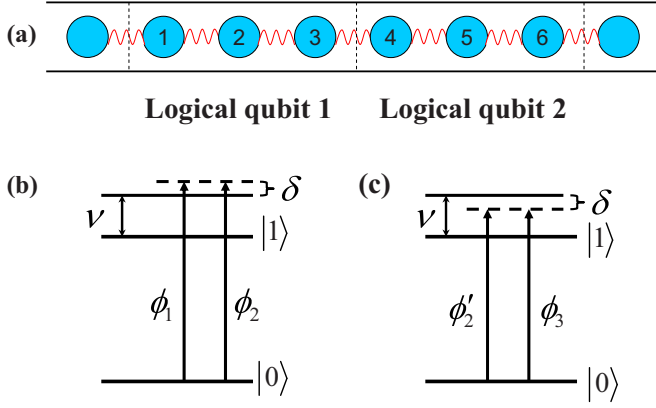


FIG. 1. (Color online) Layout for logical qubits and laser configuration. (a) A schematic illustration of the logical qubits in trapped ions. Each logical qubit consists of three ions. (b) Two lasers acting on ion 1 (2) are tuned to frequencies  $\omega_0 + (\nu + \delta)$  with phase  $\phi_1$  ( $\phi_2$ ). (c) Two lasers acting on ion 2 (3) are tuned to frequencies  $\omega_0 + (\nu - \delta)$  with the same phase  $\phi'_2 = \phi_3$ .

Hamiltonian is given by [32]

$$H^{12} = \nu a^\dagger a + \omega_0 \sum_{i=1}^2 \sigma_z^i + \left[ \Omega_{12} e^{-i\eta(a+a^\dagger)} e^{i(\omega_0 + \nu + \delta)t} \sum_{i=1}^2 \sigma_i e^{i\phi_i} + \text{H.c.} \right], \quad (1)$$

where  $\hbar = 1$  is assumed,  $a^\dagger$  and  $a$  are the creation and annihilation operators for the collective vibrational mode,  $\Omega_{12}$  stands for the Rabi frequency of the two lasers acting on ions 1 and 2,  $\eta = k/\sqrt{2\nu M}$  is the Lamb-Dicke parameter, with  $k$  being the wave vector along the trap axis and  $M$  the mass of the ion collection,  $\sigma_z^i = \frac{1}{2}(|1\rangle_i \langle 1| - |0\rangle_i \langle 0|)$ , and  $\sigma_i = |0\rangle_i \langle 1|$  where  $|0\rangle$  and  $|1\rangle$  denote the ground and excited states of an ion, respectively. In the interaction picture, under the rotating-wave approximation, and also considering the Lamb-Dicke limit  $\eta^2(n+1) \ll 1$  with  $n$  being the phonon number, the effective Hamiltonian takes the form of [6,32,33]

$$H^{12} = -i\eta\Omega_{12} \sum_{i=1}^2 \sigma_i e^{i\phi_i} a^\dagger e^{-i\delta t} + \text{H.c.} \quad (2)$$

When  $\delta \gg \eta\Omega_{12}$ , the effective Hamiltonian is given by

$$H^{12} = \frac{\eta^2\Omega_{12}^2}{\delta} \sum_{j=1}^2 (-a^\dagger a |0\rangle_i \langle 0| + a a^\dagger |1\rangle_i \langle 1|) + \frac{\eta^2\Omega_{12}^2}{\delta} (e^{i\varphi_{12}} \sigma_1 \sigma_2^+ + \text{H.c.}), \quad (3)$$

where  $\varphi_{12} = \phi_1 - \phi_2$ . When the vibrational mode is initially in the vacuum state, which has been realized in experiments [34], the effective Hamiltonian reduces to

$$H^{12} = \frac{\eta^2\Omega_{12}^2}{\delta} \sum_{j=1}^2 |1\rangle_i \langle 1| + \frac{\eta^2\Omega_{12}^2}{\delta} (e^{i\varphi_{12}} \sigma_1 \sigma_2^+ + \text{H.c.}). \quad (4)$$

Applying another classical laser, the Stark shifts can be easily compensated [35], and then the wanted effective Hamiltonian is simplified as

$$H_{XY}^{12} = \frac{\eta^2\Omega_{12}^2}{\delta} (e^{i\varphi_{12}} \sigma_1 \sigma_2^+ + \text{H.c.}). \quad (5)$$

With the laser configuration as shown in Fig. 1(c), two lasers acting on ions 2 and 3 are tuned to frequencies  $\omega_0 + (\nu - \delta)$  with the same phase  $\phi_3 = \phi'_2$ . Similarly, the wanted effective Hamiltonian  $H_{XY}^{23}$  can also be obtained as

$$H_{XY}^{23} = -\frac{\eta^2\Omega_{23}^2}{\delta} (\sigma_2 \sigma_3^+ + \text{H.c.}). \quad (6)$$

### III. ONE-QUBIT HOLONOMIC GATES

Now we turn to the construction of universal single-logical qubit operations for NHQC in DFSs. It is noted that a logical qubit consisting of two physical qubits is not sufficient to realize NHQC in DFSs for a dephasing environment [29]. So we use three physical qubits to encode a logical qubit. For three physical qubits interacting collectively with the dephasing environment, described by the interaction Hamiltonian  $H_I = S_z \otimes B$ , where  $S_z = \sum_{i=1}^3 \sigma_z^i$  is the collective dephasing operator and  $B$  is an arbitrary environment operator, there exists a three-dimensional DFS

$$S^{D_1} := \text{span}\{|100\rangle, |001\rangle, |010\rangle\}, \quad (7)$$

where the computational basis, i.e., the logical qubit states, are denoted as  $|0\rangle_L = |100\rangle$  and  $|1\rangle_L = |001\rangle$ . Meanwhile,  $|001\rangle$  is used as an ancillary state, denoted as  $|a_1\rangle = |010\rangle$  for convenience.

We now consider the implementation of single-logical qubit operations. For ions 1 and 2, we apply  $H_{XY}^{12}$  for a duration of  $T_1$ , i.e.,  $T_1$  is the entire operation time. Meanwhile, we also apply  $H_{XY}^{23}$  on ions 2 and 3 for a time  $T_1$ . Then, in the weak-field regime  $\{\eta\Omega_{12}, \eta\Omega_{23}\} \ll \delta$ , the effective Hamiltonian reads

$$H_1 = \lambda_1 \left( \sin \frac{\theta}{2} e^{i\varphi} |a_1\rangle_L \langle 0| - \cos \frac{\theta}{2} |a_1\rangle_L \langle 1| + \text{H.c.} \right), \quad (8)$$

where the effective Rabi frequency  $\lambda_1 = \frac{\eta^2}{\delta} \sqrt{|\Omega_{12}|^4 + |\Omega_{23}|^4}$ , the phase  $\varphi = \varphi_{12}$ , and the ratio  $|\Omega_{12}|^2/|\Omega_{23}|^2 = \tan(\theta/2)$  should be kept as a constant during each pulse pair. This is a so-called  $\Lambda$ -like effective Hamiltonian, with  $|a_1\rangle_L$  at the top and  $|0\rangle_L, |1\rangle_L$  at the bottom. In the dress state representation, the two degenerate states with zero eigenvalue are

$$\begin{aligned} |d\rangle_L &= \cos \frac{\theta}{2} |0\rangle_L + \sin \frac{\theta}{2} e^{i\varphi} |1\rangle_L, \\ |b\rangle_L &= \sin \frac{\theta}{2} e^{-i\varphi} |0\rangle_L - \cos \frac{\theta}{2} |1\rangle_L. \end{aligned} \quad (9)$$

The dark state  $|d\rangle_L$  decouples from the bright state  $|b\rangle_L$  and the excited state  $|a_1\rangle_L$ ; the bright state  $|b\rangle_L$  couples from the excited state  $|a_1\rangle_L$  with the effective Rabi frequency  $\lambda_1$ . The Hamiltonian  $H_1$  causes the dark state  $|d\rangle_L$  and the bright state  $|b\rangle_L$  to evolve to the states

$$\begin{aligned} |\zeta_1(t)\rangle_L &= U_1(t, 0) |d\rangle_L = |d\rangle_L, \\ |\zeta_2(t)\rangle_L &= U_1(t, 0) |b\rangle_L = \cos(\lambda_1 t) |b\rangle_L - i \sin(\lambda_1 t) |a_1\rangle_L. \end{aligned} \quad (10)$$

If the pulse length  $T_1$  is chosen to satisfy the condition of  $\lambda_1 T_1 = \pi$ , the degenerate subspace  $\{|\zeta_1(t)\rangle_L, |\zeta_2(t)\rangle_L\}$  undergoes a cyclic evolution:

$$\begin{aligned} |\zeta_1(T_1)\rangle_L \langle \zeta_1(T_1)| &= |\zeta_1(0)\rangle_L \langle \zeta_1(0)|, \\ |\zeta_2(T_1)\rangle_L \langle \zeta_2(T_1)| &= |\zeta_2(0)\rangle_L \langle \zeta_2(0)|. \end{aligned} \quad (11)$$

The final time evolution operation on the initial degenerate subspace  $\{|d\rangle_L, |b\rangle_L\}$  spanned by the computational basis states  $|0\rangle_L$  and  $|1\rangle_L$  within the Hilbert space spanned by the state vectors  $\{|0\rangle_L, |1\rangle_L, |a_1\rangle_L\}$  is written as

$$U_1(T_1, 0) = \sum_{k,l=1}^2 (\mathcal{T} e^{i \int_0^{T_1} [A(t) - H(t)] dt})_{kl} |\zeta_k(0)\rangle_L \langle \zeta_l(0)|, \quad (12)$$

where  $\mathcal{T}$  is time ordering. Here,  $A_{kl}(t) = i \langle \zeta_k(t) | \dot{\zeta}_l(t) \rangle_L$ ,  $H_{kl}(t) = \langle \zeta_k(t) | H(t) | \zeta_l(t) \rangle_L = 0$ , making the evolution satisfy the parallel-transport condition and vanishing dynamic contribution on the degenerate subspace  $\{|\zeta_1(t)\rangle_L, |\zeta_2(t)\rangle_L\}$ . As a consequence, the operation is purely geometric. Thus, the unitary on the initial degenerate subspace  $\{|d\rangle_L, |b\rangle_L\}$

$$U_1(C) = \mathcal{P} e^{i \oint_C \mathcal{A}} = \begin{pmatrix} 1 & 0 \\ 0 & -1 \end{pmatrix} \quad (13)$$

is the holonomy matrix associated with a closed path  $C$  in the base space  $G(3; 2)$ , which is the set of two-dimensional degenerate subspaces within the Hilbert space spanned by the state vectors  $\{|0\rangle_L, |1\rangle_L, |a_1\rangle_L\}$ . Here  $\mathcal{P}$  is path ordering and  $\mathcal{A} = A(t)dt$  is the connection one-form expressed as

$$\mathcal{A} = \begin{pmatrix} 0 & 0 \\ 0 & \lambda_1 dt \end{pmatrix}. \quad (14)$$

In the computational space spanned by  $\{|0\rangle_L, |1\rangle_L\}$ ,  $U_1(C)$  is the holonomic single-qubit gate

$$U_1(\theta, \varphi) = U_1(C) = \begin{pmatrix} \cos \theta & \sin \theta e^{-i\varphi} \\ \sin \theta e^{i\varphi} & -\cos \theta \end{pmatrix}, \quad (15)$$

which can be used to realize a universal set of single-logical qubit gates [27], i.e., any desired single-qubit gate can be realized by the proper choosing of  $\theta$  and  $\varphi$ . For example, when  $\theta = \frac{\pi}{4}$  and  $\varphi = 0$ , a Hadamard gate is implemented. Meanwhile one can combine  $U_1(\frac{\pi}{2}, \frac{\pi}{4})U_1(\frac{\pi}{2}, 0)$  to implement a phase gate.

The main decoherence effect in our scheme is due to the spontaneous emission from the excited states. In the following, we numerically show how the spontaneous emission affects the fidelity of the resulting gate. In principle, the implementation of a master equation is justified when the dynamics of the Liouvillian of the system is adiabatic compared to the correlation time of the environment (see, for instance, Ref. [36]). In the presence of the spontaneous emission, the evolution of the system in the Markov approximation is governed by the following Lindblad equation [37]:

$$\frac{d\rho}{dt} = -i[H_1, \rho] + \gamma \left( L\rho L^\dagger - \frac{1}{2}\rho L^\dagger L - \frac{1}{2}L^\dagger L\rho \right), \quad (16)$$

where  $\rho$  is the density operator,  $\gamma$  is the spontaneous emission rate, and  $L = \sigma_+ \otimes I \otimes I + I \otimes \sigma_+ \otimes I + I \otimes I \otimes \sigma_+$  is the Lindblad operator with  $\sigma_+ = |1\rangle\langle 0|$  and  $I$  being the lower

and identity operators of a physical qubit (ion). Taking the Hadamard gate for example, the fidelity of which is defined as  $f = [\text{tr}(\rho_a \rho_b)]^{1/2}$  with  $\rho_a(\rho_b)$  being the density operator of the system in the case with (without) decay. Based on the Lindblad equation (16),  $f$  is numerically calculated based on the Hamiltonian (8). We choose the experimentally achievable parameters as the following:  $\eta = 0.044$ ,  $\delta = 2\pi \times 20$  kHz,  $\Omega_{12} = 2\pi \times 35.4$  kHz,  $\Omega_{23} = 2\pi \times 55$  kHz, and  $\gamma = 0.8$  Hz (lifetime 1.2 s) [38,39]. These parameters apparently meet the conditions mentioned above. Our numerical simulation shows that the infidelity  $(1 - f)$  due to the spontaneous emission in a single cyclic evolution is less than 0.001. Moreover, when the control over the operation time is not exact, e.g.,  $T_1 = 1.05\pi/\lambda_1$ , there will be a small infidelity of the gate operation, which is about 0.005. This is because once the area of the pulses deviates from  $\pi$ , the state cannot completely return to the computational subspace  $\{|0\rangle_L, |1\rangle_L\}$ , i.e., the final state will have a nonzero population in the ancillary state  $|a_1\rangle_L$ . Similar infidelity will be introduced with imperfect control over the relative amplitudes and phases of the two driving fields. Therefore, accurate control over these parameters is of crucial importance to maintain the ultrahigh gate operation.

#### IV. TWO-QUBIT HOLONOMIC GATES

We next proceed to the implementation of the two-qubit controlled-phase gate. Providing the implemented arbitrary single-qubit gate, universal quantum computation can be realized. For two logical qubits interacting collectively with the dephasing environment, there exists a six-dimensional DFS [17–19]:

$$\begin{aligned} S^{D_2} := \text{span}\{ & |100100\rangle, |100001\rangle, |001100\rangle, \\ & |001001\rangle, |101000\rangle, |000101\rangle\}. \end{aligned} \quad (17)$$

We use the same encoding of the logical qubit states as that of the single-qubit case, i.e.,  $|00\rangle_L = |100100\rangle$ ,  $|01\rangle_L = |100001\rangle$ ,  $|10\rangle_L = |001100\rangle$ , and  $|11\rangle_L = |001001\rangle$ . However, the remaining vectors  $|a_2\rangle = |101000\rangle$  and  $|a_3\rangle = |000101\rangle$  both used as ancillary states, are not the combination of the single-qubit basis. Giving the fact that single-logical qubit operations will not affect  $|a_2\rangle$  and  $|a_3\rangle$ , single-qubit operations will not introduce additional error with this six-dimensional DFS for two-qubit operations.

Two lasers acting on ions 3 and 4 are tuned to frequencies  $\omega_0 + (v + \delta)$  with phase  $\phi'_3$  and phase  $\phi_4$ , respectively. We apply  $H_{XY}^{34}$  for a time  $T_2$ .  $T_2$  is the operation time. At the same time, two lasers acting on ions 3 and 6 are tuned to frequencies  $\omega_0 + (v - \delta)$  with the same phase  $\phi_6$ . We also apply  $H_{XY}^{36}$  for a time  $T_2$ . The effective Hamiltonian then reads

$$\begin{aligned} H_2 = \lambda_2 \left\{ \sin \frac{\vartheta}{2} e^{i\xi} (|a_2\rangle_L \langle 00| + |a_3\rangle_L \langle 11|) \right. \\ \left. - \cos \frac{\vartheta}{2} (|a_2\rangle_L \langle 01| + |a_3\rangle_L \langle 10|) + \text{H.c.} \right\}, \end{aligned} \quad (18)$$

where the effective Rabi frequency  $\lambda_2 = \frac{\eta^2}{\delta} \sqrt{|\Omega_{34}|^4 + |\Omega_{36}|^4}$ , the phase  $\xi = \varphi_{34} = \phi'_3 - \phi_4$ , and the ratio  $|\Omega_{34}|^2/|\Omega_{36}|^2 = \tan(\vartheta/2)$  should be kept as a constant during each pulse pair.

The Hamiltonian  $H_2$  can be decomposed as

$$H_2 = \lambda_2(H^{(0)} + H^{(1)}). \quad (19)$$

The two terms are

$$H^{(0)} = \sin \frac{\vartheta}{2} e^{i\xi} |a_2\rangle_L \langle 00| - \cos \frac{\vartheta}{2} |a_2\rangle_L \langle 01| + \text{H.c.}, \quad (20)$$

$$H^{(1)} = \sin \frac{\vartheta}{2} e^{i\xi} |a_3\rangle_L \langle 11| - \cos \frac{\vartheta}{2} |a_3\rangle_L \langle 10| + \text{H.c.},$$

and they are commutative, which implies that

$$e^{-i \int_0^{T_2} H_2 dt} = e^{-i\pi H^{(0)}} e^{-i\pi H^{(1)}} \quad (21)$$

under the  $\pi$  pulse criterion  $\lambda_2 T_2 = \pi$ . The factor  $e^{-i\pi H^{(0)}}$  and  $e^{-i\pi H^{(1)}}$  of the time-evolution operator in (21) acts nontrivially on the computational subspaces  $\{|00\rangle_L, |01\rangle_L\}$  and  $\{|10\rangle_L, |11\rangle_L\}$ , respectively. Thus,  $H_2$  effectively reduces to two  $\Lambda$ -like Hamiltonians: one with  $|a_2\rangle_L$  at the top and  $|00\rangle_L, |01\rangle_L$  at the bottom and the other with  $|a_3\rangle_L$  at the top and  $|10\rangle_L, |11\rangle_L$  at the bottom. The holonomic two-logical qubit gate in the subspace  $\{|00\rangle_L, |01\rangle_L, |10\rangle_L, |11\rangle_L\}$  reads as

$$U_2(\vartheta, \xi) = \begin{pmatrix} \cos \vartheta & \sin \vartheta e^{-i\xi} & 0 & 0 \\ \sin \vartheta e^{i\xi} & -\cos \vartheta & 0 & 0 \\ 0 & 0 & -\cos \vartheta & \sin \vartheta e^{i\xi} \\ 0 & 0 & \sin \vartheta e^{-i\xi} & \cos \vartheta \end{pmatrix}, \quad (22)$$

following the analogy of the single-qubit gate above.

In the following, we prove that  $U_2(\vartheta, \xi)$  acts as an entangling gate within the DFS. We combine single- and two-qubit logical gates to implement the entangling controlled- $U$  gate within the chosen DFS. First, we act  $U_2(\vartheta, \xi)$  on logical qubits 1 and 2. Secondly, we act  $U_1(\theta, \varphi)$  on logical qubit 1 with  $\theta = \vartheta$  and  $\varphi = \xi$ . Then, an entangling controlled- $U$  gate is implemented, which is

$$U_c(\vartheta, \xi) = |0\rangle_{L_1} \langle 0| \otimes I_{L_2} + |1\rangle_{L_1} \langle 1| \otimes U(\vartheta, \xi), \quad (23)$$

where  $U(\vartheta, \xi)$  has a matrix representation of

$$U(\vartheta, \xi) = \begin{pmatrix} \sin^2 \vartheta e^{2i\xi} - \cos^2 \vartheta & -\sin 2\vartheta \cos \xi \\ \sin 2\vartheta \cos \xi & \sin^2 \vartheta e^{-2i\xi} - \cos^2 \vartheta \end{pmatrix}. \quad (24)$$

When  $\vartheta = \frac{\pi}{2}$ , the entangling controlled-phase-shift gate  $U_{CP}(\xi)$  ( $\xi \neq k\pi/2, k = 0, 1, \dots$ ) with matrix representation

$$U_{CP}(\xi) = \begin{pmatrix} 1 & 0 & 0 & 0 \\ 0 & 1 & 0 & 0 \\ 0 & 0 & e^{2i\xi} & 0 \\ 0 & 0 & 0 & e^{-2i\xi} \end{pmatrix} \quad (25)$$

is implemented within the chosen DFS (see Fig. 2).

In the following, we numerically show how the spontaneous emission affects the fidelity of the entangling controlled-phase gate  $U_{CP}(\pi/4)$ , which is implemented by the combination of  $U_2(\pi/2, \pi/4)$  and  $U_1(\pi/2, \pi/4)$ . The fidelity of a single logical qubit gate has been estimated at the end of Sec. III, and thus we just simulate the fidelity of the holonomic two-logical qubit gate  $U_2(\pi/2, \pi/4)$  under the spontaneous emission. The

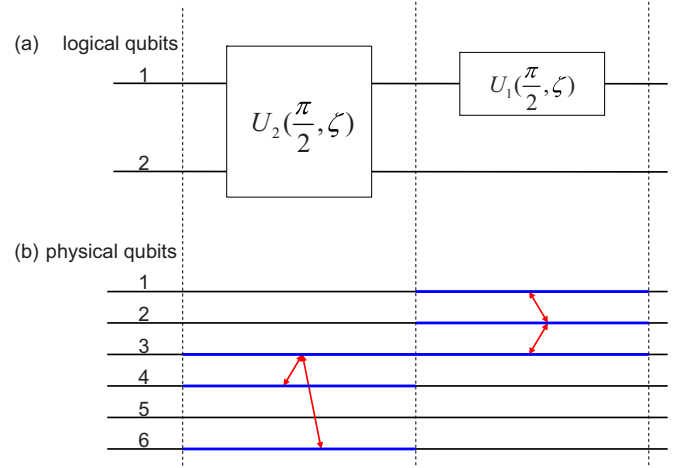


FIG. 2. (Color online) Pulse sequence to realize a controlled-phase gate  $U_{CP}(\xi)$  within the DFS. (a) The logical pulse sequence. (b) The operations on the physical qubits. The arrows represent the  $H_{XY}$  interaction between two physical qubits  $U_2(\frac{\pi}{2}, \xi)$ . Acting on logical qubits 1 and 2 requires ion 3 to interact with ion 4 and ion 3 to interact with ion 6 simultaneously.  $U_1(\frac{\pi}{2}, \xi)$  acting on logical qubit 1 requires ion 1 to interact with ion 2 and ion 2 to interact with ion 3 simultaneously.

fidelity of the  $U_2(\pi/2, \pi/4)$  is defined as  $f' = [\text{tr}(\rho'_a \rho'_b)]^{1/2}$  with  $\rho'_a$  ( $\rho'_b$ ) being the density operator of the system in the case with (without) spontaneous emission. Based on the Lindblad master equation similar to Eq. (16) but in the case of two logical qubits, the fidelity of the  $U_2(\pi/2, \pi/4)$  gate,  $f'$ , is numerically simulated based on the Hamiltonian (18). With the same parameters as in the single-qubit gate case, our simulation shows that the infidelity  $(1 - f')$  due to the spontaneous emission in a single cyclic evolution is less than 0.002.

## V. CONCLUSION

In summary, we have proposed a scheme for implementing NHQC in DFSs with trapped ions, and have shown how to realize universal quantum computation by using two-body pairwise effective exchange interactions only. In comparison to the previous scheme [29], our proposal seems easier to physically implement under current technology in ion traps [30,38]. Based on the fact that universal quantum computation in DFSs has been realized with trapped ions very recently [30], our scheme seems promising in experimental implementation with high fidelities, by combining the resilience of the DFSs approach against collective noises and the robustness of NHQC against local noises.

## ACKNOWLEDGMENTS

We thank X. D. Zhang and S. L. Zhu for their helpful discussions. This work was supported by the NSF of China (Grant No. 11104085), the Major Research Plan of the NSF of China (Grant No. 91121023), the NFRPC (Grant No. 2013CB921804), FOYTHEG(Yq2013050), PRNPGZ(2014010), and PCSIRT(IRT1243). D.Y.X. was also supported by the SRFGS of SCNU.

- [1] E. Sjöqvist, *Physics* **1**, 35 (2008).
- [2] P. Zanardi and M. Rasetti, *Phys. Lett. A* **264**, 94 (1999); J. Pachos, P. Zanardi, and M. Rasetti, *Phys. Rev. A* **61**, 010305(R) (1999).
- [3] L.-M. Duan, J. I. Cirac, and P. Zoller, *Science* **292**, 1695 (2001).
- [4] Wang Xiang-Bin and M. Keiji, *Phys. Rev. Lett.* **87**, 097901 (2001).
- [5] S. L. Zhu and Z. D. Wang, *Phys. Rev. Lett.* **89**, 097902 (2002); *Phys. Rev. A* **66**, 042322 (2002); **67**, 022319 (2003); X. D. Zhang, S. L. Zhu, L. Hu, and Z. D. Wang, *ibid.* **71**, 014302 (2005).
- [6] S. L. Zhu and Z. D. Wang, *Phys. Rev. Lett.* **91**, 187902 (2003); S. L. Zhu, Z. D. Wang, and P. Zanardi, *ibid.* **94**, 100502 (2005).
- [7] Y. Shi, *Europhys. Lett.* **83**, 50002 (2008); X. Li and Y. Shi, *ibid.* **102**, 40011 (2013); Z. S. Wang, C. Wu, X. L. Feng, L. C. Kwek, C. H. Lai, C. H. Oh, and V. Vedral, *Phys. Rev. A* **76**, 044303 (2007); G. W. Lin, X. B. Zou, X. M. Lin, and G. C. Guo, *ibid.* **79**, 064303 (2009).
- [8] Z.-Y. Xue and Z. D. Wang, *Phys. Rev. A* **75**, 064303 (2007); Z.-Y. Xue, Z. D. Wang, and S.-L. Zhu, *ibid.* **77**, 024301 (2008); Z.-Y. Xue, *Quantum Inf. Process.* **11**, 1381 (2012).
- [9] X. Tan, D. W. Zhang, Z. Zhang, Y. Yu, S. Han, and S. L. Zhu, *Phys. Rev. Lett.* **112**, 027001 (2014); J. Zhang, J. Zhang, X. Zhang, and K. Kim, *Phys. Rev. A* **89**, 013608 (2014).
- [10] D. Leibfried, B. DeMarco, V. Meyer, D. Lucas, M. Barrett, J. Britton, W. M. Itano, B. Jelenković, C. Langer, T. Rosenband, and D. J. Wineland, *Nature (London)* **422**, 412 (2003); J. Du, P. Zou, and Z. D. Wang, *Phys. Rev. A* **74**, 020302(R) (2006).
- [11] A. A. Abdumalikov, Jr., J. M. Fink, K. Juliusson, M. Pechal, S. Berger, A. Wallraff, and S. Filipp, *Nature (London)* **496**, 482 (2013).
- [12] G. Feng, G. Xu, and G. Long, *Phys. Rev. Lett.* **110**, 190501 (2013).
- [13] A. Recati, T. Calarco, P. Zanardi, J. I. Cirac, and P. Zoller, *Phys. Rev. A* **66**, 032309 (2002).
- [14] L. Faoro, J. Siewert, and R. Fazio, *Phys. Rev. Lett.* **90**, 028301 (2003).
- [15] V. N. Golovach, M. Borhani, and D. Loss, *Phys. Rev. A* **81**, 022315 (2010).
- [16] K. Toyoda, K. Uchida, A. Noguchi, S. Haze, and S. Urabe, *Phys. Rev. A* **87**, 052307 (2013).
- [17] L. M. Duan and G. C. Guo, *Phys. Rev. Lett.* **79**, 1953 (1997).
- [18] P. Zanardi and M. Rasetti, *Phys. Rev. Lett.* **79**, 3306 (1997).
- [19] D. A. Lidar, I. L. Chuang, and K. B. Whaley, *Phys. Rev. Lett.* **81**, 2594 (1998).
- [20] P. G. Kwiat, A. J. Berglund, J. B. Altepeter, and A. G. White, *Science* **290**, 498 (2000).
- [21] D. Kielpinski, V. Meyer, M. A. Rowe, C. A. Sackett, W. M. Itano, C. Monroe, and D. J. Wineland, *Science* **291**, 1013 (2001).
- [22] M. Mohseni, J. S. Lundeen, K. J. Resch, and A. M. Steinberg, *Phys. Rev. Lett.* **91**, 187903 (2003).
- [23] J. E. Ollerenshaw, D. A. Lidar, and L. E. Kay, *Phys. Rev. Lett.* **91**, 217904 (2003).
- [24] M. Bourennane, M. Eibl, S. Gaertner, C. Kurtsiefer, A. Cabello, and H. Weinfurter, *Phys. Rev. Lett.* **92**, 107901 (2004).
- [25] J. K. Pachos and A. Beige, *Phys. Rev. A* **69**, 033817 (2004); X. L. Feng, C. F. Wu, H. Sun, and C. H. Oh, *Phys. Rev. Lett.* **103**, 200501 (2009); Z.-Y. Xue, S.-L. Zhu, and Z. D. Wang, *Eur. Phys. J. D* **55**, 223 (2009).
- [26] P. Zanardi, *Phys. Rev. Lett.* **87**, 077901 (2001); L. A. Wu, P. Zanardi, and D. A. Lidar, *ibid.* **95**, 130501 (2005); Z. R. Zhang, C. Y. Li, C. W. Wu, H. Y. Dai, and C. Z. Li, *Phys. Rev. A* **86**, 042320 (2012).
- [27] E. Sjöqvist, D. M. Tong, L. M. Andersson, B. Hessmo, M. Johansson, and K. Singh, *New J. Phys.* **14**, 103035 (2012).
- [28] V. A. Mousolou, C. M. Canali, and E. Sjöqvist, *New J. Phys.* **16**, 013029 (2014).
- [29] G. F. Xu, J. Zhang, D. M. Tong, E. Sjöqvist, and L. C. Kwek, *Phys. Rev. Lett.* **109**, 170501 (2012).
- [30] T. Monz, K. Kim, A. S. Villar, P. Schindler, M. Chwalla, M. Riebe, C. F. Roos, H. Häffner, W. Hänsel, M. Hennrich, and R. Blatt, *Phys. Rev. Lett.* **103**, 200503 (2009).
- [31] C. Monroe and J. Kim, *Science* **339**, 1164 (2013); R. Blatt and D. Wineland, *Nature (London)* **453**, 1008 (2008).
- [32] A. Sørensen and K. Mølmer, *Phys. Rev. Lett.* **82**, 1971 (1999); *Phys. Rev. A* **62**, 022311 (2000).
- [33] S. L. Zhu, C. Monroe, and L. M. Duan, *Phys. Rev. Lett.* **97**, 050505 (2006); *Europhys. Lett.* **73**, 485 (2006).
- [34] F. Schmidt-Kaler, H. Häffner, M. Riebe, S. Gulde, G. P. T. Lancaster, T. Deuschle, C. Becher, C. F. Roos, J. Eschner, and R. Blatt, *Nature (London)* **422**, 408 (2003); M. Riebe, K. Kim, P. Schindler, T. Monz, P. O. Schmidt, T. K. Körber, W. Hänsel, H. Häffner, C. F. Roos, and R. Blatt, *Phys. Rev. Lett.* **97**, 220407 (2006).
- [35] H. Häffner, S. Gulde, M. Riebe, G. Lancaster, C. Becher, J. Eschner, F. Schmidt-Kaler, and R. Blatt, *Phys. Rev. Lett.* **90**, 143602 (2003).
- [36] G. Florio, P. Facchi, R. Fazio, V. Giovannetti, and S. Pascazio, *Phys. Rev. A* **73**, 022327 (2006); D. Parodi, M. Sassetti, P. Solinas, P. Zanardi, and N. Zanghì, *ibid.* **73**, 052304 (2006).
- [37] G. Lindblad, *Commun. Math. Phys.* **48**, 119 (1976).
- [38] J. Benhelm, G. Kirchmair, C. F. Roos, and R. Blatt, *Nat. Phys.* **4**, 463 (2008).
- [39] P. A. Barton, C. J. S. Donald, D. M. Lucas, D. A. Stevens, A. M. Steane, and D. N. Stacey, *Phys. Rev. A* **62**, 032503 (2000).